JOURNAL OF MATERIALS SCIENCE 11 (1976) 71–77

Identification of the initial stage sintering mechanism using aligned wires

R. M. GERMAN
Metallurgy and Electroplating Division 8312, Sandia Laboratories, Livermore, California, USA

Z. A. MUNIR
Materials and Devices Research Group, Department of Mechanical Engineering, University of California, Davis, California, USA

The introduction of a new kinetic parameter for monitoring morphology changes during wire–wire sintering is proposed. It is shown that the specific pore–solid perimeter of a cross-sectioned wire bundle has a characteristic dependence on neck size. Thus, the perimeter, which is suitable for quantitative metallographic analysis, becomes a means of determining the sintering rate and mechanism. Analyses of Cu and Au data using this technique illustrate its advantages and accuracy. The kinetics of gold wire sintering are analysed with the aid of available diffusion data. It is concluded that the sintering of gold is a multiple diffusion process involving volume, surface and possibly grain-boundary paths. The importance of each mechanism is discussed with respect to particle size, neck size, and temperature.

1. Introduction

Sintering mechanism identification has traditionally relied on the neck size growth rate [1]. Variations [2–8] of this original Kuczynski treatment have not substantially altered the following relationship describing the isothermal neck growth between two spheres or wires:

$$\left(\frac{x}{a}\right)^n = Bt. \quad (1)$$

As indicated by Fig. 1, x/a is the neck radius divided by the particle (wire) radius, n is the mechanism characteristic exponent, t is the isothermal sintering time, and B is a constant involving temperature, material properties, and particle size. Thus, typically the predominant mass transport process during sintering can be identified by the value of n. For bulk-transport sintering (volume diffusion, grain-boundary diffusion, plastic and viscous flow) shrinkage provides an alternative morphology parameter. However, for the surface-transport processes of surface diffusion, evaporation-condensation and volume diffusion from the surface, no similar parameter is available. Recent morphology modelling by the authors has provided a link between neck size and the specific surface area during sintering [9, 10]. The approach has been to model the interparticle neck with a minimum surface area configuration which satisfies volume conservation while also providing the appropriate curvature gradient. The shapes generated by these considerations agree quite well with those derived from flux equations for surface diffusion controlled sintering. Similar comparisons for the

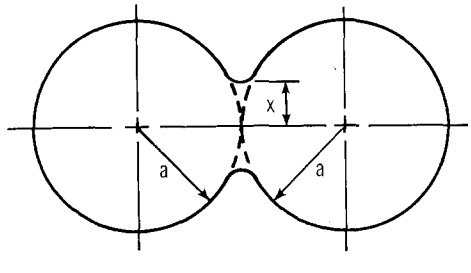

Figure 1 Schematic diagram illustrating neck growth between either two spheres or two wires at an intermediate point in the sintering process.

bulk transport processes are not possible. However, such geometric comparisons as provided by the surface area, neck size, and shrinkage agree with available experimental data. The modelling results show that the specific surface area is a universal alternative to neck size during sintering studies. Thus, interpretation of sintering kinetics can be accomplished by monitoring surface area reduction. Introduction of time dependence into the surface area reduction has provided a means of identifying the operative mass-transport process [11]. Analyses of experimental data under the guidelines of the technique have demonstrated its accuracy while further substantiating the underlying neck shape models [12].

Model analysis of neck growth kinetics is often performed through use of wire bundles [13–18]. Aligned wires have several unique advantages, foremost among these are ease of preparation and subsequent analysis. However, this technique is not without shortcomings. Straining of the wires during bundle fabrication can enhance plastic flow and neck distortion, and uneven wire contacts give rise to experimental difficulties. In spite of these difficulties, wire sintering studies represent an important means of isolating the dominant mass transport mechanism for a given set of conditions. Thus, almost all sintering studies have been extended to include aligned wires.

Recent calculations [19] have provided the first precise geometrical relations during wire sintering, considering both bulk and surface-transport processes. It was shown that the pore–solid perimeter of a cross-sectioned wire bundle was a universal morphology parameter. It is the purpose of the present analysis to consider the introduction of kinetics into the pore–solid perimeter reduction. The development will closely resemble that previously employed in the sphere–sphere case [11]. Furthermore, experimental data on Cu and Au wires (the latter being generated during this investigation) will be considered in the light of the proposed model.

2. The model

In the geometric modelling of sintering wires, it was shown that the specific surface area had a characteristic dependence on the neck size and wire packing (co-ordination) [19]. The specific pore–solid perimeter in a cross-sectioned wire bundle is equivalent to the specific surface area. This equivalence makes analysis and study of wire compacts an easy task with automatic metallographic instruments. The parabolic dependence of P/P_0 (the instantaneous perimeter divided by the initial perimeter) on the neck size during the first stage of sintering indicates a possible linear relation between log $(\Delta P/P_0)$ and log (x/a). Plots of the perimeter reduction $(\Delta P/P_0)$, versus neck size on a log–log basis are shown in Figs. 2 and 3 for various

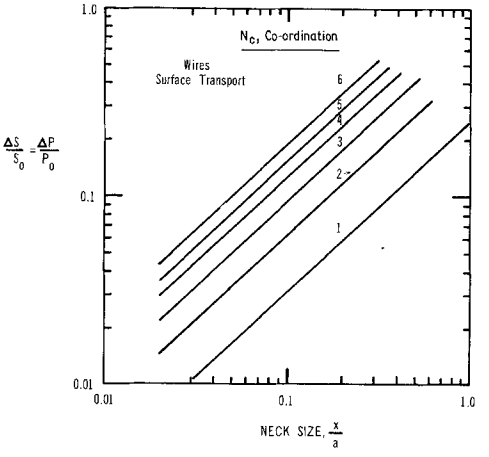

Figure 2 Perimeter reduction $\Delta P/P_0$ as a function of neck size and packing co-ordination during surface-transport sintering.

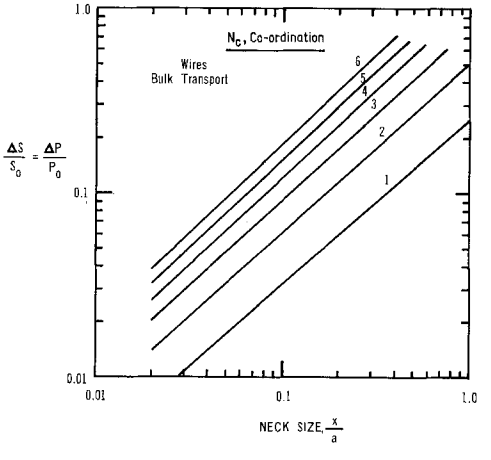

Figure 3 Perimeter reduction $\Delta P/P_0$ as a function of neck size and packing co-ordination during bulk-transport sintering.

coordinations. This linearization holds with less than 2% error over the range shown. However, the slopes do vary with wire co-ordination, N_c. Physically, a wire co-ordination of six corresponds to the closest packing of equal sized wires, while a packing of two would represent a plane of aligned wires. From these results the dependence of the

specific perimeter reduction on neck size can be expressed as

$$\frac{\Delta P}{P_0} = K\left(\frac{x}{a}\right)^m \tag{2}$$

where K and m are constants for a given experiment. Shown in Fig. 4 are the variations of K and m with transport mechanism (bulk versus surface) and wire co-ordination. The subscripts S and B refer to surface and bulk transport, processes, respectively. Interestingly, the exponential constant m, is relatively insensitive to wire co-ordination for the surface transport case.

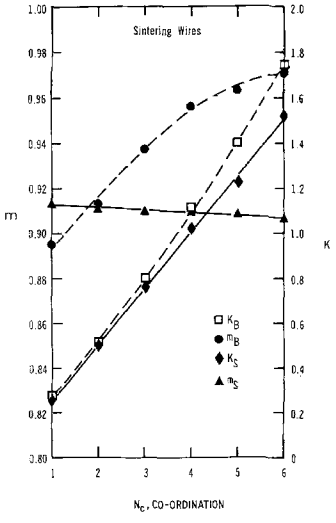

Figure 4 Dependence of the constants K and m of Equation 2 on wire co-ordination and transport class (B = bulk and S = surface).

Combining Equations 1 and 2 allows introduction of time dependence into the perimeter reduction. Thus,

$$\frac{\Delta P}{P_0} = K(Bt)^{m/n} \tag{3}$$

or, alternatively

$$\left(\frac{\Delta P}{P_0}\right)^{n/m} = K't \tag{4}$$

where $K' = BK^{n/m}$. Equation 4 is generally valid up to $\Delta P/P_0$ values of 50%. The identification of the initial stage sintering mechanism for aligned wires can, therefore, be accomplished through the kinetics of the pore–solid perimeter reduction. Experimentally, this can be achieved through monitoring the specific perimeter reduction and comparing the slope of log $(\Delta P/P_0)$ versus log t with the predicted values listed in Table I. The time dependent relations of Kuczynski [1, 18], Rockland [6, 7], Kingery and Berg [3], Coble [4], and Frenkel [20], have been used in arriving at the values listed in constructing this table. Critical reviews by numerous authors have led to their general acceptance [6, 7, 18, 21–24].

3. Application to previous results

Perimeter reduction in wire compacts is not generally reported. Alexander and Balluffi [13] have measured the rugosity coefficient during isothermal sintering of 128 μm copper wires. The rugosity coefficient is proportional to the pore–solid perimeter per pore during the initial sintering stage. When pores become circular the relation between perimeter and rugosity breaks down. However, this case exceeds the limit of applicability of the present model. Shown in Fig. 5 is the $\Delta P/P_0$ data of Alexander and Balluffi for copper at 1000° C. Also shown in this figure is the neck size and shrinkage data for the same experiment. The inverse slope n of the neck size time dependence is 5.6, and the corresponding values derived from the shrinkage and perimeter reduction are 6.1 and 6.2, respectively. Although these time dependencies represent a scatter about a value of six, a general

TABLE I Kinetic exponents for the wire–wire perimeter reduction

Mechanism	n	n/m			Shrinkage
		$N_c = 2$	$N_c = 4$	$N_c = 6$	
Plastic or viscous flow	2	2.2	2.1	2.1	yes
Evaporation-condensation	3	3.3	3.3	3.3	no
Volume diffusion	5	5.5	5.2	5.1	yes*
Grain-boundary diffusion	6	6.6	6.3	6.2	yes
Surface diffusion	7	7.7	7.7	7.7	no

*Assuming densification, see remarks of Rockland [7].

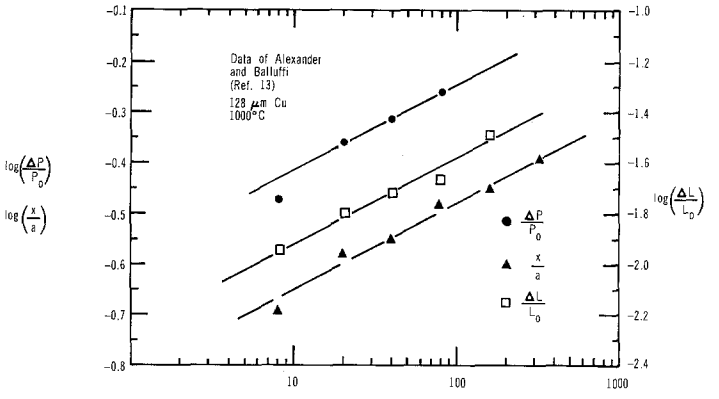

Figure 5 Data of Alexander and Balluffi showing the comparison of sintering kinetic parameters.

agreement is evident. Alexander and Balluffi concluded that volume diffusion was the mechanism for sintering. In the light of our analysis this conclusion is somewhat doubtful. It seems more plausible that these data represent the combined action of volume and surface diffusion, and the variations in the calculated time dependencies result from too few datum points. Rockland [7] has offered essentially the same multiple mechanism explanation for his studies on copper spheres (125 μm diameter) sintering at 1050° C.

4. Experimental

Since the data available for testing the present kinetic model are limited, a series of experiments using aligned gold wires were conducted. Gold wires of 137 μm average diameter and a purity of 99.999%* were coiled around a 1.5 cm diameter high purity alumina cylinder. The cylinder was placed in an alumina boat in the end of a stainless steel tube. A continuous 0.5 cm^3 (STP) sec^{-1} flow of argon, which had been passed through a bed of titanium chips at 800° C, was maintained through

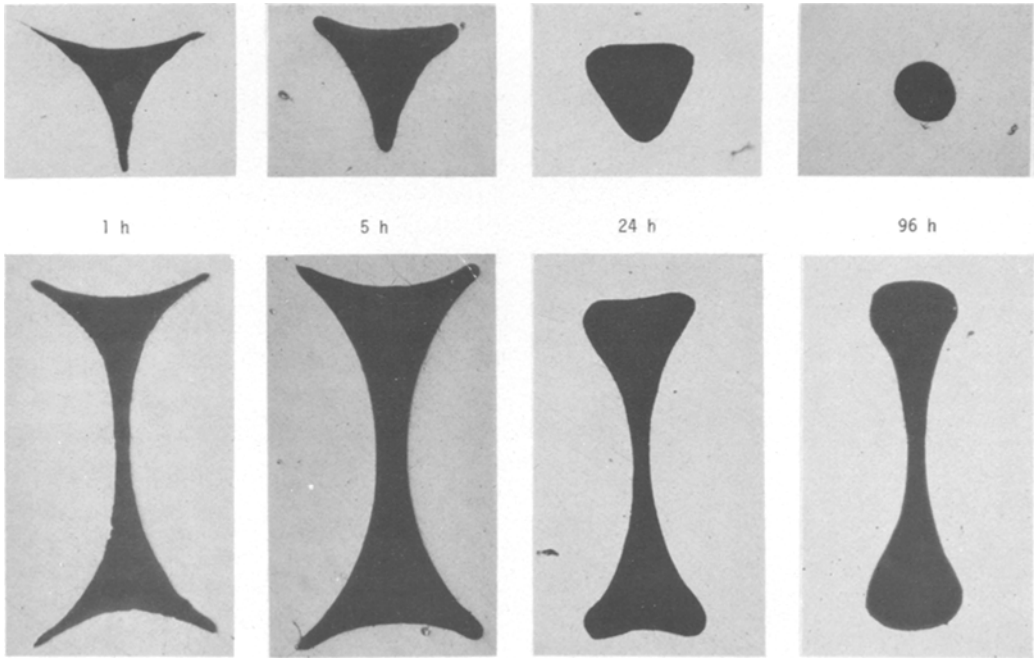

Figure 6 Changes in pore shape and size during the sintering of aligned gold wires at 1000° C.

*Obtained from Materials Research Corporation, Orangeburg, NY.

this tube. A silicon carbide furnace was positioned such that the specimen could be inserted directly into the hot zone. The furnace and tube assembly were preheated to 1000° C and allowed to stabilize at this temperature under continuous argon flow. Temperature was measured with two Pt/Pt–10% Rh thermocouples, and was held within ± 5° C of 1000° C. After the furnace had stabilized, the gold wound alumina cylinder was inserted. This technique provided for nearly instantaneous heating and cooling of the sample. Periodically, the sample was removed and a segment cut for metallographic analysis. Specimens with elapsed times of 1, 2, 3, 5, 10, 24, 51 and 96 h were gathered by this means. These specimens were vacuum mounted in epoxy resin, ground and polished. To prevent distortion of the soft gold, final polishing was accomplished by alternating successively less severe aqua regia etches with magnesia polishings. Photomicrographs were used to make neck size and pore–solid perimeter measurements. Typically, 30 to 100 microstructural features were measured for an individual datum point. Both pores of co-ordinations four and six were observed in the compacts and their perimeters tallied separately. The techniques outlined by Underwood [25] were found satisfactory for making perimeter measurements quickly and easily.

5. Results

Example photomicrographs showing pore rounding and contraction are shown in Fig. 6 for both co-ordinations. Neck size and perimeter reduction are plotted as functions of time in Figs. 7 and 8, respectively. Typical scatter in the data about the mean for both parameters was ± 10%. Least squares fit to the averaged neck sizes gave a time dependency of 6.4. As shown in Fig. 7, the data are in good agreement with such a linearization. The inverse slopes of Fig. 8 for the perimeter reduction are 6.2 and 6.3, for $N_c = 6$ and 4, respectively. Since shrinkage did occur during the experiment the corresponding time dependencies are calculated to be 6.0 and 6.1 (see Fig. 4). These values are in reasonable agreement with that determined by neck size measurement. The $N_c = 4$ pores tended to be elongated rather than uniaxial. Such a pore shape departs significantly from that assumed in the original model. Interestingly, this difference had a minimal effect on the time dependence.

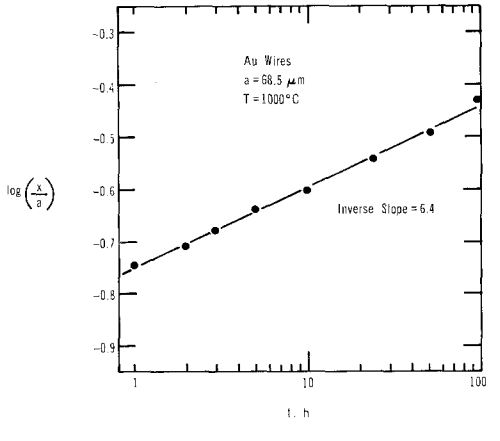

Figure 7 Neck size as a function of time for aligned gold wires at 1000° C.

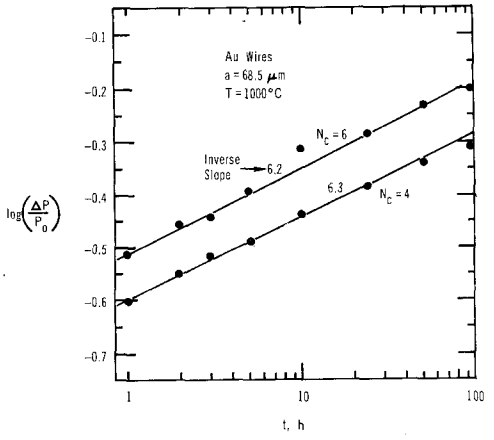

Figure 8 Perimeter reduction shown as a function of sintering time for aligned gold wires in packing co-ordinations of four and six.

6. Discussion

The data from this experiment as well as those from Alexander and Balluffi [13] can be compared with the model used for these calculations. In Fig. 9, the pore–solid perimeter reduction $\Delta P/P_0$, is plotted as a function of neck size x/a. Both the Au and Cu experimental data are compared with the predictions of the proposed model [19]. The good agreement between the experimental data and the predicted values of the model affirms the validity of the assumed neck profile. Furthermore, an added advantage of the proposed approach is its adaptability to automatic image analysis techniques. Multiple measurements can be made in a non-tedious manner to obtain statistical confidence.

With regard to the gold sintering data, a time dependence between six and seven is indicative of multiple diffusional processes. Undoubtedly, surface diffusion is a major contributor to mass flow. In fact, previous low temperature studies [26, 27]

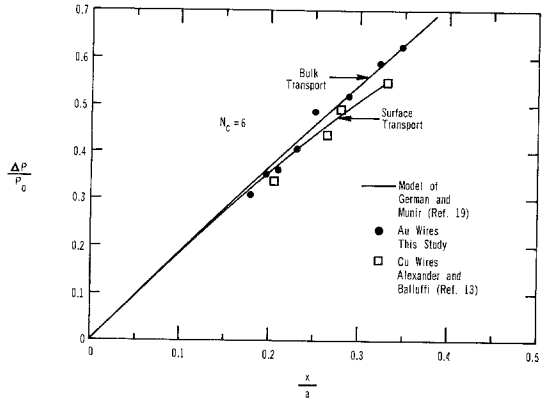

Figure 9 Comparison of experimental data with the neck size-perimeter relation of German and Munir [19].

on small gold spheres showed surface diffusion to be the dominant sintering mechanism. However, temperature and particle size dependence indicates volume diffusion will become more significant as particle size and temperature are increased. The role played by grain-boundary diffusion is difficult to ascertain due to insufficient diffusion data. Estimates of the grain-boundary diffusion coefficient at 1000° C based on silver data and gold in copper data would place D_G between 10^{-5} and $10^{-7}\,cm^2\,sec^{-1}$ [28]. The surface diffusion coefficient D_s, lies between 6×10^{-4} and $6 \times 10^{-5}\,cm^2\,sec^{-1}$ at 1000° C [29, 30]. However, surface contamination can substantially alter the surface diffusion coefficient [26, 27]. Tracer studies on the volume diffusion coefficient of gold place D_v at $6.5 \times 10^{-9}\,cm^2\,sec^{-1}$ at 1000° C [31–33]. Using the ratio of rates technique [34, 35], the rates of neck growth by various processes can be compared. That is, for volume and surface diffusion

$$\frac{\dot{x}_v}{\dot{x}_s} \cong \frac{8}{5}\frac{aD_v}{\delta D_s}\left(\frac{x}{a}\right)^2 \qquad (5)$$

where $\dot{x}_v$ is the neck growth rate by volume diffusion, $\dot{x}_s$ is the neck growth rate by surface diffusion, and δ is the interatomic spacing. Substituting the appropriate values into this equation shows that both mechanisms were contributing significantly to neck growth at 1000° C. Similarly the ratio of neck growth rates by surface and grain-boundary diffusion processes

$$\frac{\dot{x}_G}{\dot{x}_s} \cong \frac{16D_B}{D_s}\left(\frac{x}{a}\right) \qquad (6)$$

suggests that grain-boundary diffusion also contributes to gold sintering at 1000° C. These considerations substantiate the non-integral time dependence as determined in this experiment. Thus, it is concluded that surface and volume diffusion transport modes are active sintering processes for gold at 1000° C. The relative dominance of volume diffusion increases with particle size, temperature and neck growth. The importance of grain-boundary diffusion cannot be established at this time due to imprecise diffusion coefficient estimates.

One technique often employed to identify the sintering mechanism is to measure the temperature dependence of the sintering rate. Typically, a simple Arrhenius process is assumed. The experimentally determined activation energy is then compared with those for the various diffusion processes to identify the rate controlling mechanism. Unfortunately, such comparisons can be misleading. When significant mass flow is occurring by more than one mechanism, these calculations result in large activation energies. The temperature sensitivity of the diffusivities, and hence the rate ratios of Equations 5 and 6 further complicate this approach. Hence, variable temperature experiments would not aid in the present discussion.

7. Conclusions

The introduction of sintering kinetics into previously published morphology relations has provided a new sintering parameter for aligned wires. The specific perimeter reduction has proved to be an accurate monitor of sintering. The specific perimeter reduction (equivalent to the specific surface area reduction for aligned wires) provides a new means of determining the sintering time dependency. Analysis by automatic quantitative metallography instruments is available for the specific perimeter, but not for the previously used neck size. Thus, a reliable technique for sintering studies is available. Copper and gold wire compacts have been analysed by this technique to demonstrate its usefulness. Available diffusion data for the gold system indicates sintering is a multiple mechanism process involving surface diffusion, volume diffusion and quite likely grain-boundary diffusion.

Acknowledgements

The authors are indebted to C.W.Karfs of Sandia Laboratories for his care in preparing the metallographic samples. This work was supported by the Energy Research and Development Administration under Contract Number AT-(29-1)-789.

References

1. G. C. KUCZYNSKI, *Trans. Met. Soc. AIME* **185** (1949) 169.
2. B. Ya. PINES, *Usp. Fiz. Naukssr.* **52** (1954) 501.
3. W. D. KINGERY and M. BERG, *J. Appl. Phys.* **26** (1955) 1205.
4. R. L. COBLE, *J. Amer. Ceram. Soc.* **41** (1958) 55.
5. D. L. JOHNSON and I. B. CUTLER, *ibid* **46** (1963) 541.
6. J. G. R. ROCKLAND, *Acta Met.* **14** (1966) 1273.
7. *Idem, ibid* **15** (1967) 277.
8. B. Ya. PINES and A. F. SIRENKO, *Fiz. Metal. Metalloved.* **28** (1969) 832.
9. R. M. GERMAN and Z. A. MUNIR, *Met. Trans.* **6B** (1975) 289.
10. *Idem, ibid* **6A**, December (1975).
11. *Idem*, "A Kinetic Model for the Reduction in Surface Area During the Initial Stage of Sintering", presented at the Fourth Notre Dame Conference on Sintering and Related Phenomena, May 1975.
12. *Idem*, "The Identification of the Initial-Stage Sintering Mechanism: A New Approach", presented at the Fourth Notre Dame Conference on Sintering and Related Phenomena, May 1975.
13. B. H. ALEXANDER and R. W. BALLUFFI *Acta Met.* **5** (1958) 666.
14. A. L. PRANATIS and L. SEIGLE, "Powder Metallurgy", edited by W. Leszynski (Interscience, New York, 1961) p. 53.
15. H. ICHINOSE and G. C. KUCZYNSKI, *Acta Met.* **10** (1962) 209.
16. J. BRETT and L. SEIGLE, *ibid* **14** (1966) 575.
17. G. D. RIECK and J. G. R. ROCKLAND, Planseeberichte Fur Pulvermetallurgie, **13** (1965) 3.
18. G. C. KUCZYNSKI, *Adv. Colloid Interface Sci.* **3** (1972) 275.
19. R. M. GERMAN and Z. A. MUNIR, *J. Mater. Sci.* **10** (1975) 1719.
20. J. FRENKEL, *J. Phys. USSR*, **9** (1954) 385.
21. D. L. JOHNSON, *J. Amer. Ceram. Soc.* **53** (1970) 574.
22. M. M. RISTIC, *Phys. Sintering* **1** (1969) A1.
23. F. THUMMLER and W. THOMMA, *Met. Rev.* **12** (1967) 69.
24. J. R. MOON, *Powder Met. Int.* **3** (1971), 147, 194.
25. E. E. UNDERWOOD, "Quantitative Stereology" (Addison-Wesley, Reading, Mass., 1970) p. 36.
26. D. W. PASHLEY, M. J. STOWELL, M. H. JACOBS and T. J. LAW, *Phil. Mag.* **10** (1965) 127.
27. K. H. OLSEN and G. C. NICHOLSON, *J. Amer. Ceram. Soc.* **51** (1968) 669.
28. H. GLEITER and B. CHALMERS, "High-Angle Grain Boundaries", Progress in Materials Science, Vol. 16 (Pergamon Press, New York, 1972).
29. M. McLEAN and J. P. HIRTH, *Surf. Sci.* **12** (1968) 177.
30. N. A. GJOSTEIN, *Trans. Met. Soc. AIME* **236** (1966) 1267; **239** (1967) 785.
31. S. M. MAKIN, A. H. ROWE and A. D. LeCLAIRE, *Proc. Phys. Soc.* **B70** (1957) 545.
32. D. DUHL, K. HIRANO and M. COHEN, *Acta Met.* **11** (1963) 1.
33. H. M. GILDER and D. LAZARUS, *J. Phys. Chem. Solids* **26** (1965) 2081.
34. L. L. SEIGLE, *Prog. Powder Met.* **20** (1965) 221.
35. T. L. WILSON and P. G. SHEWMON, *Trans. Met. Soc. AIME* **236** (1966) 48.

Received 12 May and accepted 26 June 1975.